

## Isomers in $^{128}\text{Pd}$ and $^{126}\text{Pd}$ : Evidence for a Robust Shell Closure at the Neutron Magic Number 82 in Exotic Palladium Isotopes

H. Watanabe,<sup>1,2,3,\*</sup> G. Lorusso,<sup>3</sup> S. Nishimura,<sup>3</sup> Z. Y. Xu,<sup>4</sup> T. Sumikama,<sup>5</sup> P.-A. Söderström,<sup>3</sup> P. Doornenbal,<sup>3</sup> F. Browne,<sup>3,6</sup> G. Gey,<sup>3,7</sup> H. S. Jung,<sup>8,†</sup> J. Taprogge,<sup>3,9,10</sup> Zs. Vajta,<sup>3,11</sup> J. Wu,<sup>3,12</sup> A. Yagi,<sup>13</sup> H. Baba,<sup>3</sup> G. Benzoni,<sup>14</sup> K. Y. Chae,<sup>15</sup> F. C. L. Crespi,<sup>14,16</sup> N. Fukuda,<sup>3</sup> R. Gernhäuser,<sup>17</sup> N. Inabe,<sup>3</sup> T. Isobe,<sup>3</sup> A. Jungclaus,<sup>10</sup> D. Kameda,<sup>3</sup> G. D. Kim,<sup>18</sup> Y. K. Kim,<sup>18,19</sup> I. Kojouharov,<sup>20</sup> F. G. Kondev,<sup>21</sup> T. Kubo,<sup>3</sup> N. Kurz,<sup>20</sup> Y. K. Kwon,<sup>18</sup> G. J. Lane,<sup>22</sup> Z. Li,<sup>12</sup> C.-B. Moon,<sup>23</sup> A. Montaner-Pizá,<sup>24</sup> K. Moschner,<sup>25</sup> F. Naqvi,<sup>26</sup> M. Niikura,<sup>4</sup> H. Nishibata,<sup>13</sup> D. Nishimura,<sup>27</sup> A. Odahara,<sup>13</sup> R. Orlandi,<sup>28</sup> Z. Patel,<sup>29</sup> Zs. Podolyák,<sup>29</sup> H. Sakurai,<sup>3</sup> H. Schaffner,<sup>20</sup> G. S. Simpson,<sup>7</sup> K. Steiger,<sup>17</sup> H. Suzuki,<sup>3</sup> H. Takeda,<sup>3</sup> A. Wendt,<sup>25</sup> and K. Yoshinaga<sup>27</sup>

<sup>1</sup>International Research Center for Nuclei and Particles in the Cosmos, Beihang University, Beijing 100191, China

<sup>2</sup>School of Physics and Nuclear Energy Engineering, Beihang University, Beijing 100191, China

<sup>3</sup>RIKEN Nishina Center, 2-1 Hirosawa, Wako, Saitama 351-0198, Japan

<sup>4</sup>Department of Physics, University of Tokyo, Hongo, Bunkyo-ku, Tokyo 113-0033, Japan

<sup>5</sup>Department of Physics, Tohoku University, Aoba, Sendai, Miyagi 980-8578, Japan

<sup>6</sup>School of Computing Engineering and Mathematics, University of Brighton, Brighton BN2 4GJ, United Kingdom

<sup>7</sup>LPSC, Institut National Polytechnique de Grenoble, Université Joseph Fourier Grenoble 1, CNRS/IN2P3, F-38026 Grenoble Cedex, France

<sup>8</sup>Department of Physics, Chung-Ang University, Seoul 156-756, Republic of Korea

<sup>9</sup>Departamento de Física Teórica, Universidad Autónoma de Madrid, E-28049 Madrid, Spain

<sup>10</sup>Instituto de Estructura de la Materia, CSIC, E-28006 Madrid, Spain

<sup>11</sup>MTA Atomki, P.O. Box 51, Debrecen H-4001, Hungary

<sup>12</sup>Department of Physics, Peking University, Beijing 100871, China

<sup>13</sup>Department of Physics, Osaka University, Machikaneyama-machi 1-1, Osaka 560-0043 Toyonaka, Japan

<sup>14</sup>INFN, Sezione di Milano, via Celoria 16, I-20133 Milano, Italy

<sup>15</sup>Department of Physics, Sungkyunkwan University, Suwon 440-746, Republic of Korea

<sup>16</sup>Dipartimento di Fisica, Università di Milano, via Celoria 16, I-20133 Milano, Italy

<sup>17</sup>Physik Department, Technische Universität München, D-85748 Garching, Germany

<sup>18</sup>Rare Isotope Science Project, Institute for Basic Science, Daejeon 305-811, Republic of Korea

<sup>19</sup>Department of Nuclear Engineering, Hanyang University, Seoul 133-791, Republic of Korea

<sup>20</sup>GSI Helmholtzzentrum für Schwerionenforschung GmbH, 64291 Darmstadt, Germany

<sup>21</sup>Nuclear Engineering Division, Argonne National Laboratory, Argonne, Illinois 60439, USA

<sup>22</sup>Department of Nuclear Physics, Research School of Physical Sciences and Engineering, Australian National University, Canberra, A.C.T 0200, Australia

<sup>23</sup>Department of Display Engineering, Hoseo University, Chung-Nam 336-795, Republic of Korea

<sup>24</sup>IFIC, CSIC-Universidad de Valencia, A.C. 22085, E 46071 Valencia, Spain

<sup>25</sup>Institut für Kernphysik, Universität zu Köln, Zùlpicher Strasse 77, D-50937 Köln, Germany

<sup>26</sup>Wright Nuclear Structure Laboratory, Yale University, New Haven, Connecticut 06520-8120, USA

<sup>27</sup>Department of Physics, Faculty of Science and Technology, Tokyo University of Science, 2641 Yamazaki, Noda, Chiba, Japan

<sup>28</sup>Instituut voor Kern en Stralingsfysica, KU Leuven, University of Leuven, B-3001 Leuven, Belgium

<sup>29</sup>Department of Physics, University of Surrey, Guildford GU2 7XH, United Kingdom

(Received 9 August 2013; published 8 October 2013)

The level structures of the very neutron-rich nuclei  $^{128}\text{Pd}$  and  $^{126}\text{Pd}$  have been investigated for the first time. In the  $r$ -process waiting-point nucleus  $^{128}\text{Pd}$ , a new isomer with a half-life of  $5.8(8) \mu\text{s}$  is proposed to have a spin and parity of  $8^+$  and is associated with a maximally aligned configuration arising from the  $g_{9/2}$  proton subshell with seniority  $\nu = 2$ . For  $^{126}\text{Pd}$ , two new isomers have been identified with half-lives of  $0.33(4)$  and  $0.44(3) \mu\text{s}$ . The yrast  $2^+$  energy is much higher in  $^{128}\text{Pd}$  than in  $^{126}\text{Pd}$ , while the level sequence below the  $8^+$  isomer in  $^{128}\text{Pd}$  is similar to that in the  $N = 82$  isotone  $^{130}\text{Cd}$ . The electric quadrupole transition that depopulates the  $8^+$  isomer in  $^{128}\text{Pd}$  is more hindered than the corresponding transition in  $^{130}\text{Cd}$ , as expected in the seniority scheme for a semimagic, spherical nucleus. These experimental findings indicate that the shell closure at the neutron number  $N = 82$  is fairly robust in the neutron-rich Pd isotopes.

DOI: [10.1103/PhysRevLett.111.152501](https://doi.org/10.1103/PhysRevLett.111.152501)

PACS numbers: 23.35.+g, 23.20.Lv, 27.60.+j

The concept of magicity and its underlying shell structures is of supreme importance for many-body fermionic systems in a confined space. For instance, the noble gases are chemically inert because they have closed-shell configurations of electrons. Another well-known example is the clustering phenomena observed for metal ions [1], which can form supershells with the specific numbers of atoms. It is recognized that shell structures arise from the quantized motion of the constituent fermions in a mean-field potential with rotational invariance [2].

In the case of atomic nuclei, there are two types of fermions (nucleons), proton and neutron, both of which can have magic numbers. While the bunching of the single-particle energy levels at nucleon numbers 2, 8, and 20 could be reproduced with a simple (spherically symmetric) harmonic oscillator potential, it was realized that a strong spin-orbit interaction plays a significant role in the emergence of heavier magic numbers 28, 50, 82, and 126 [3,4]. For the last few decades, however, the study of exotic nuclei using radioactive isotope (RI) beams revealed that the aforementioned magic numbers, which have been empirically confirmed for nuclei near the  $\beta$ -stability line, are not necessarily universal and are subjected to a change in some regions with highly asymmetric proton number ( $Z$ ) and neutron number ( $N$ );  $^{12}\text{Be}$  ( $N = 8$ ) [5],  $^{32}\text{Mg}$  ( $N = 20$ ) [6], and  $^{42}\text{Si}$  ( $N = 28$ ) [7] are known to be deformed in consequence of erosion of the respective neutron shell gaps. Such a paradigm shift is one of the frontier issues in nuclear physics, and whether it will also take place at the heavier traditional magic numbers is an open question worth investigating.

The present work focuses on neutron-rich nuclei below the doubly magic nucleus  $^{132}\text{Sn}$  ( $Z = 50$ ,  $N = 82$ ). It has been suggested by a self-consistent mean-field theory that the  $N = 82$  spherical shell gap gradually decreases approaching the neutron drip line due to the combined effect of weak binding in largely diffused neutron densities and strong pairing-induced coupling between bound orbitals and low- $\ell$  continuum states [8]. In the region of interest, albeit far inward from the drip line, a high  $Q_\beta$  value observed for the decay of  $^{130}\text{Cd}$  ( $Z = 48$ ,  $N = 82$ ) was consistent with mass-model predictions assuming a shell quenching at  $N = 82$  [9]. Contrary to this, the yrast level sequence below the  $8^+$  isomer in  $^{130}\text{Cd}$  can be interpreted in a shell-model framework that does not consider excitations across the shell gaps, indicating no evidence for the shell quenching in this nucleus [10]. From an astrophysical point of view, it has been argued that the property of the  $N = 82$  shell closure far from the valley of  $\beta$ -stability affects the Solar System abundance pattern particularly around the prominent  $A \approx 130$  peak in the  $r$ -process nucleosynthesis [11], and, hence, a proper understanding of the underlying nuclear structure of the  $r$ -process isotopes is highly required.

In this Letter, we present the first spectroscopic results on  $^{128}\text{Pd}$  ( $Z = 46$ ,  $N = 82$ ) and  $^{126}\text{Pd}$  ( $N = 80$ ), the former of which is a waiting point nucleus on the  $r$ -process path. Since the discovery of these isotopes at the RI Beam Factory (RIBF) facility at RIKEN [12,13], steady improvements in the intensity of uranium beams, in combination with a highly efficient  $\gamma$ -ray detection system, enable us to conduct detailed spectroscopic studies.

Neutron-rich nuclei below  $^{132}\text{Sn}$  were produced using in-flight fission of a  $^{238}\text{U}^{86+}$  beam at 345 MeV/nucleon, incident on a beryllium target with a thickness of 3 mm. The primary beam intensity ranged from 7 to 12 pA during the experiments. The nuclei of interest were separated and transported through the BigRIPS and ZeroDegree spectrometers [14], operated with wedge-shaped aluminum degraders with thicknesses of 2.9 and 2.5 mm at the first and second dispersive focal planes, respectively, for purification of the secondary beams. Identification of particles with the atomic number ( $Z$ ) and the mass-to-charge ratio ( $A/q$ ) was achieved on the basis of the  $\Delta E$ -TOF- $B\rho$  method, in which the energy loss ( $\Delta E$ ), time of flight (TOF), and magnetic rigidity ( $B\rho$ ) were measured using the focal plane detectors on the beam line. The obtained particle-identification spectrum is shown in Ref. [15]. About  $1.1 \times 10^3$  and  $6.5 \times 10^4$  ions were collected for  $^{128}\text{Pd}$  and  $^{126}\text{Pd}$ , respectively.

The identified particles were implanted into a highly segmented active stopper, named WAS3ABi [16], which consisted of eight double-sided silicon-strip detectors (DSSSD) stacked compactly. Each DSSSD had a thickness of 1 mm with an active area segmented into sixty and forty strips (1-mm pitch) on each side in the horizontal and vertical dimensions, respectively. The DSSSDs also served as detectors for electrons following  $\beta$ -decay and internal conversion processes. Gamma rays were detected by the EURICA spectrometer [16], which consisted of twelve Cluster-type detectors, each of which contained seven HPGe crystals packed closely, which were developed for the former EUROBALL array [17].

Figure 1(a) shows a  $\gamma$ -ray energy spectrum measured in delayed coincidence with  $^{128}\text{Pd}$  ions. Four  $\gamma$  rays at energies of 75, 260, 504, and 1311 keV have been unambiguously observed. These  $\gamma$  rays are found to be in mutual coincidence [see Fig. 1(b) as an example] and exhibit consistent time behavior. Therefore, we conclude that they proceed through a single cascade originating from one isomeric state. A least-squares fit of the summed gated time spectra of the isomeric-decay transitions yields  $T_{1/2} = 5.8(8) \mu\text{s}$  half-life as demonstrated in Fig. 2(a). The relative intensities of these isomeric  $\gamma$  rays, which are listed in the fifth column of Table I, are in agreement within experimental errors, except for the 75-keV transition that is expected to be highly converted. The total internal conversion coefficient for the 75-keV transition derived from a comparison with the 1311-keV  $\gamma$ -ray

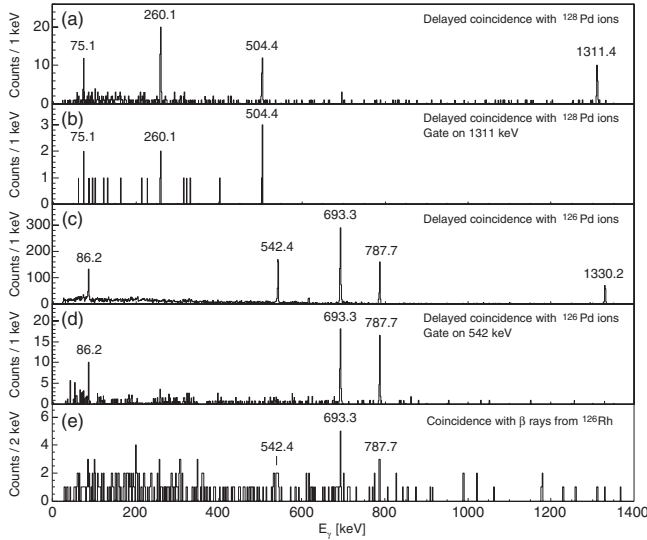


FIG. 1. Gamma-ray spectra measured (a) in coincidence with  $^{128}\text{Pd}$  ions within a time range of 0.15–25  $\mu\text{s}$ , (b) additionally, with a gate on the 1311-keV line, (c) in coincidence with  $^{126}\text{Pd}$  ions within 0.15–5  $\mu\text{s}$ , (d) additionally, with a gate on the 542-keV line, (e) in coincidence with  $\beta$  rays detected within 100 ms after the implantation of  $^{126}\text{Rh}$  ions.

intensity is 2.6(17), which is consistent with the theoretical value of 3.88 for an  $E2$  multipolarity.

On the basis of the above arguments on the observed  $\gamma$  transitions, the level scheme of  $^{128}\text{Pd}$  is proposed as displayed in Fig. 3, where the spin and parity of the 5.8- $\mu\text{s}$  isomeric state at 2151 keV is assigned as  $J^\pi = 8^+$ . The spin-parity assignment for the levels and the ordering of the transitions between the isomer and the ground state are based on a close resemblance to the yrast level sequences below the analogous  $8^+$  isomers in  $^{130}\text{Cd}$  [10] and  $^{96}\text{Pd}$  ( $N = 50$ ) [18]. A transition strength of  $B(E2; 8^+ \rightarrow 6^+) = 0.22(3)$  W.u. can be obtained from the measured half-life of the 2151-keV isomeric state.

The level scheme of  $^{126}\text{Pd}$  constructed in the current work is also shown in Fig. 3. The 693-keV  $\gamma$  ray, which is the most intense peak of those observed in delayed

coincidence with  $^{126}\text{Pd}$  ions (Fig. 1(c)), is assigned as the  $2^+ \rightarrow 0^+$  transition; this assignment is supported by the observation of a prominent  $\gamma$ -ray peak at the same energy in the  $\beta$  decay of  $^{126}\text{Rh}$ , which was also included in the cocktail beam, as shown in Fig. 1(e). The coincidence spectrum with a gate on the 542-keV  $\gamma$  ray [Fig. 1(d)] clearly exhibits  $\gamma$  rays at energies of 693, 788, and 86 keV, but not at 1330 keV, indicating that two parallel cascades stem from a common level at 2023 keV. The assignment of transitions below the 2023-keV level is affirmed by the observed  $\gamma$ -ray intensities, namely,  $I_{542} \approx I_{788}$  and  $I_{693} \approx I_{788} + I_{1330}$ ; see Table I. The 86-keV transition is placed just above the 2023-keV level, because this  $\gamma$  ray was observed to precede all the four transitions.

As shown in Figs. 2(b) and 2(c), a half-life of 0.44(3)  $\mu\text{s}$  is derived from the time distribution of the 86-keV  $\gamma$  ray relative to the beam implantation, while the time difference between the 86-keV  $\gamma$  ray and the subsequent transitions provides  $T_{1/2} = 0.33(4)$   $\mu\text{s}$ . Thus, it is found that two isomeric states lie at 2023 and 2110 keV. The assignment of spins and parities for the two isomeric states is based on the  $\gamma$ -ray feeding pattern and transition probabilities. Given the  $J^\pi = 5^-$  and  $7^-$  assignments for the 2023- and 2110-keV levels, respectively, the strengths of the isomeric decay transitions are  $B(E1; 5^- \rightarrow 4^+) = 2.9(4) \times 10^{-9}$  W.u. (542 keV),  $B(E3; 5^- \rightarrow 2^+) = 0.24(3)$  W.u. (1330 keV), and  $B(E2; 7^- \rightarrow 5^-) = 2.13(14)$  W.u. (86 keV). These strengths are comparable with the values of the corresponding transitions in the  $N = 80$  isotope  $^{128}\text{Cd}$  [19]. These negative parity isomers might be (weakly) populated in the  $\beta$  decay of  $^{126}\text{Rh}$ , as the 542- and 788-keV  $\gamma$  rays seem to appear in Fig. 1(e).

As is evident from Fig. 3, the level structure of  $^{128}\text{Pd}$  is quite different from that of  $^{126}\text{Pd}$ . One of the remarkable features is a sudden increase in the yrast  $2^+$  energy from 693 keV in  $N = 80$  to 1311 keV in  $N = 82$ . Correspondingly, the energy ratio  $R_{4/2} = E(4^+)/E(2^+)$  decreases from 2.14, a value consistent with a typical vibrational interpretation, to 1.38, being characteristic of

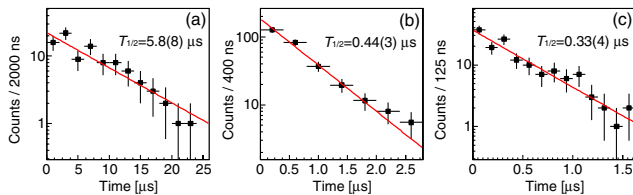


FIG. 2 (color online). (a) Sum of the time distributions of the 260-, 504-, and 1311-keV  $\gamma$  rays in  $^{128}\text{Pd}$ . (b) Time spectrum of the 86-keV  $\gamma$  ray in  $^{126}\text{Pd}$ . (c) Time difference between the 86-keV transition and  $\gamma$  rays below the isomer at 2023 keV in  $^{126}\text{Pd}$ . The horizontal and vertical bars on the data points represent the width of time bins and the statistical errors, respectively. The solid lines represent the results of a least-squares fit.

TABLE I. Summary of transitions and measured half-lives of the excited states in  $^{128}\text{Pd}$  and  $^{126}\text{Pd}$ . The relative intensities of  $\gamma$  rays are extracted from the  $\gamma$ -ray energy spectra shown in Figs. 1(a) and 1(c) for  $^{128}\text{Pd}$  and  $^{126}\text{Pd}$ , respectively.

	$E_x$ (keV)	$T_{1/2}$	$E_\gamma$ (keV)	$I_\gamma$ (%)	$J_i^\pi \rightarrow J_f^\pi$
$^{128}\text{Pd}$	1311.4		1311.4	100(29)	$(2^+) \rightarrow 0^+$
	1815.8		504.4	88(24)	$(4^+) \rightarrow (2^+)$
	2075.9		260.1	74(20)	$(6^+) \rightarrow (4^+)$
	2151.0	5.8(8) $\mu\text{s}$	75.1	28(10)	$(8^+) \rightarrow (6^+)$
$^{126}\text{Pd}$	693.3		693.3	100(5)	$(2^+) \rightarrow 0^+$
	1481.0		787.7	57(4)	$(4^+) \rightarrow (2^+)$
	2023.4	0.33(4) $\mu\text{s}$	542.4	52(3)	$(5^-) \rightarrow (4^+)$
			1330.2	40(3)	$(5^-) \rightarrow (2^+)$
	2109.7	0.44(3) $\mu\text{s}$	86.2	21(2)	$(7^-) \rightarrow (5^-)$

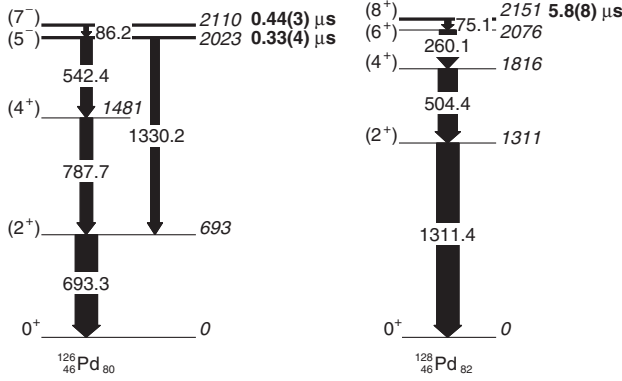


FIG. 3. Partial level schemes of  $^{126}\text{Pd}$  (left) and  $^{128}\text{Pd}$  (right) established in the present work. The widths of arrows represent relative intensities of  $\gamma$  rays summarized in Table I.

a two-quasiparticle excitation in single closed-shell nuclei, as the neutron number increases. These features for the low-lying yrast levels suggest that the  $N = 82$  shell gap persists in the Pd isotopes.

The excitation energies of the  $J^\pi = 2^+ - 8^+$  states in  $^{128}\text{Pd}$  are comparable to those in  $^{130}\text{Cd}$  [10], as demonstrated in Fig. 4(a). The constancy of level energies is characteristic of the seniority scheme [20], where seniority  $\nu$  counts the number of nucleons that are not in pairs coupled to spin zero. In case of a  $n$ -particle (or  $n$ -hole) system in a single- $j$  shell, the level energies with identical  $J^\pi$  and  $\nu$  are independent of  $n$ . As shown in Fig. 4(a), such energy properties are also visible for the even  $N = 50$  isotones from Mo ( $Z = 42$ ) to Cd ( $Z = 48$ ), in which the yrast  $J^\pi = 2^+ - 8^+$  levels consist of the same multiplet that involves predominantly valence protons in the  $\pi g_{9/2}$  orbital with  $\nu = 2$  [21]. The gradual increase in energy as moving away from  $^{100}\text{Sn}$  ( $Z = 50$ ) reflects the lowering of the  $\nu = 0$  ground state due to the admixture of valence proton pairs in the  $p_{1/2,3/2}$  and  $f_{5/2}$  orbitals which locate below the  $g_{9/2}$  subshell. Since the single-proton levels in the  $Z = 28 - 50$  shell are nearly identical in the  $^{132}\text{Sn}$  and  $^{100}\text{Sn}$  regions [21], it is expected that the  $N = 82$  isotones exhibit similar level properties within the valence proton space to the  $N = 50$  case. Therefore, the excited states in

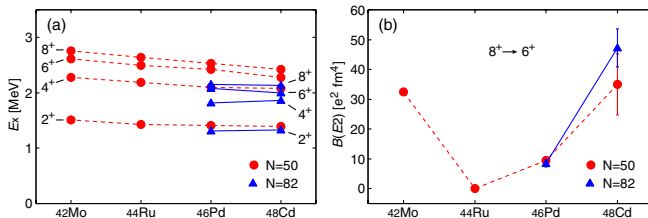


FIG. 4 (color online). Excitation energies of the yrast  $2^+ - 8^+$  states (a) and  $B(E2; 8^+ \rightarrow 6^+)$  values (b) in  $N = 50$  (filled circles) and  $N = 82$  (filled triangles) isotones. The data are taken from Ref. [28] for  $^{92}\text{Mo}$ - $^{94}\text{Ru}$ - $^{96}\text{Pd}$ , Ref. [29] for  $^{98}\text{Cd}$ , Ref. [10] for  $^{130}\text{Cd}$ , and the present work for  $^{128}\text{Pd}$ .

$^{128}\text{Pd}$  can be interpreted in terms of the  $\nu = 2$  configuration of the  $\pi g_{9/2}$  subshell.

A direct implication of the  $N = 82$  shell closure can be corroborated from the behavior of the  $E2$  transition strength for the  $8^+ \rightarrow 6^+$  isomer decay in  $^{128}\text{Pd}$ . The  $E2$  matrix elements between  $\nu = 2$  states are close to zero near the middle of the valence shell in semimagic nuclei, giving rise to seniority isomerism [20]. In Fig. 4(b), a set of measured  $B(E2; 8^+ \rightarrow 6^+)$  values for the  $N = 50$  isotones exhibits a parabolic-shape distribution as a function of the proton number due to the seniority cancellation. Meanwhile, the  $B(E2)$  value is more susceptible to configuration mixing than the level energy. If the shell gap decreases, strong proton-neutron interactions are likely to induce excitations across the closed cores and drive the system to more collective behavior. Accordingly, the  $B(E2)$  trend may deviate from the expectation of the seniority scheme. For the  $N = 82$  isotones, however, it turns out that the  $B(E2; 8^+ \rightarrow 6^+)$  value is much smaller in  $^{128}\text{Pd}$  than in  $^{130}\text{Cd}$  [Fig. 4(b)], as expected in the exact seniority classification, namely,  $B(E2; \nu = 2, n = 4) = (1/9)B(E2; \nu = 2, n = 2)$ . This observation indicates that both the  $J^\pi = 8^+$  and  $6^+$  states in the  $N = 82$  isotones, as well as in the  $N = 50$  nuclei, have good seniority  $\nu = 2$  in the well isolated  $\pi g_{9/2}$  subshell, in consequence of the robust shell closure.

The presence of the seniority isomer with  $J^\pi = 8^+$ ,  $\nu = 2$  ( $8_{\nu=2}^+$ ) in  $^{128}\text{Pd}$  is evidence for a robust shell closure at  $N = 82$ . Indeed, seniority isomerism is sensitive to the nature of underlying closed cores. This argument can be illuminated in comparison with the level systematics of even Ni ( $Z = 28$ ) isotopes with  $N = 42 - 48$ , in which valence neutrons predominantly occupy the  $\nu g_{9/2}$  orbit. The  $8_{\nu=2}^+$  isomers have been identified in  $^{70,76}\text{Ni}$  [22,23], but this is not the case for  $^{72,74}\text{Ni}$  [24]. The absence of seniority isomers in nuclei near the middle of the  $\nu g_{9/2}$  subshell can be explained by the existence of the  $6_{\nu=4}^+$  state below the  $8_{\nu=2}^+$  level, resulting in a fast  $E2$  transition between the states with different seniority [25,26]. For  $^{72}\text{Ni}$ , the authors of Ref. [27] proposed a tentative state at 2590 keV as the  $8_{\nu=2}^+$  level, which fed the  $6_{\nu=4}^+$  state at 2392 keV with an increased  $B(E2)$  value, consistent with the above mentioned seniority picture. It has been suggested that the lowering of the  $\nu = 4$  levels, as well as the fact that the energies of the yrast  $2^+$  states in  $^{70-76}\text{Ni}$  are systematically (250 ~ 400 keV) lower than those of the  $N = 50$  valence mirrors, is a signature of the softness of the  $Z = 28$  shell closure [25]. In Ref. [26], Isacker indicated that the quadrupole pairing matrix element in the relevant two-body interaction plays a significant role to determine the relative position of the  $\nu = 2$  and 4 states, and presented the conditions for the existence of the  $8_{\nu=2}^+$  isomer in a  $(g_{9/2})^4$  system. In the case of the  $N = 82$  nuclei, based on the approximation of an isolated  $g_{9/2}$  subshell, the excitation energies of the four-proton hole



nucleus are estimated to be 1347, 1810, 2051, 2118 keV for the  $2_{v=2}^+$ ,  $4_{v=2}^+$ ,  $6_{v=2}^+$ ,  $8_{v=2}^+$  states and 2184, 2455 keV for the  $4_{v=4}^+$ ,  $6_{v=4}^+$  states, using the yrast energy spectrum of  $^{130}\text{Cd}$  [10]. This estimation indicates that the  $6_{v=4}^+$  ( $6_{v=2}^+$ ) state is higher (lower) in energy than the  $8_{v=2}^+$  level, consistent with the present experimental result that the seniority isomer appears in  $^{128}\text{Pd}$ .

In conclusion, we have studied the level structures of  $^{128}\text{Pd}$  and  $^{126}\text{Pd}$ , the most neutron-rich palladium isotopes for which spectroscopic information on the excited states has been obtained to date. Inspection of the yrast  $2^+$  energy and  $E(4^+)/E(2^+)$  ratio for these nuclei, as well as the  $B(E2)$  value for the decay from the  $8^+$  seniority isomer in  $^{128}\text{Pd}$ , indicates the robustness of the  $N = 82$  shell closure for  $Z = 46$ . In future experiments, of particular interest will be to see how the seniority isomerism occur in lighter  $N = 82$  isotones  $^{126}\text{Ru}$  and  $^{124}\text{Mo}$ , which are closer to the neutron drip line.

We are indebted to the facility crews who provided the beams at RIBF, cooperated by RIKEN Nishina Center and CNS, University of Tokyo, the EUROBALL Owners Committee for the loan of germanium detectors, the PreSpec Collaboration for the use of the readout electronics. Part of the WAS3ABi was supported by the Rare Isotope Science Project which is funded by MSIP and NRF of Korea. H. S. J. was supported by the Priority Centers Research Program in Korea (2009-0093817). Zs. V. was supported by OTKA Contract No. K100835. F. G. K. was supported by the U.S. Department of Energy, Office of Nuclear Physics, under Contract No. DE-AC02-06CH11357. We acknowledge financial support from the Spanish Ministerio de Ciencia e Innovación under Contracts No. FPA2009-13377-C02 and No. FPA2011-29854-C04. We thank Prof. P. Van Isacker, Prof. K. Ogawa, and Dr. Y. Utsuno for valuable discussions and Prof. Y. Gono for warm encouragement. This work was supported by JSPS KAKENHI Grant No. 24740188.

\*Corresponding author.

hiroshi@ribf.riken.jp

†Present address: Department of Physics, University of Notre Dame, Notre Dame, Indiana 46556, USA.

- [1] W. Knight, K. Clemenger, W. de Heer, W. Saunders, M. Chou, and M. Cohen, *Phys. Rev. Lett.* **52**, 2141 (1984).
- [2] A. Bohr and B.R. Mottelson, *Nuclear Structure* (Benjamin, Reading, MA, 1975), Vol. II, p. 578.
- [3] M. G. Mayer, *Phys. Rev.* **75**, 1969 (1949).
- [4] O. Haxel, J. Jensen, and H. Suess, *Phys. Rev.* **75**, 1766 (1949).
- [5] H. Iwasaki *et al.*, *Phys. Lett. B* **481**, 7 (2000).
- [6] T. Motobayashi *et al.*, *Phys. Lett. B* **346**, 9 (1995).
- [7] B. Bastin *et al.*, *Phys. Rev. Lett.* **99**, 022503 (2007).
- [8] J. Dobaczewski, W. Nazarewicz, T. Werner, J. Berger, C. Chinn, and J. Dechargé, *Phys. Rev. C* **53**, 2809 (1996).
- [9] I. Dillmann *et al.*, *Phys. Rev. Lett.* **91**, 162503 (2003).
- [10] A. Jungclaus *et al.*, *Phys. Rev. Lett.* **99**, 132501 (2007).
- [11] K.-L. Kratz, B. Pfeiffer, O. Arndt, S. Hennrich, and A. Wöhr (t ISOLDE/IS333 Collaboration and IS393 Collaboration), *Eur. Phys. J. A* **25**, 633 (2005).
- [12] T. Ohnishi *et al.*, *J. Phys. Soc. Jpn.* **77**, 083201 (2008).
- [13] T. Ohnishi *et al.*, *J. Phys. Soc. Jpn.* **79**, 073201 (2010).
- [14] T. Kubo, *Nucl. Instrum. Methods Phys. Res., Sect. B* **204**, 97 (2003).
- [15] G. Lorusso *et al.*, RIKEN Accel. Prog. Rep. (to be published).
- [16] S. Nishimura, *Prog. Theor. Exp. Phys.* **2012**, 03C006 (2012).
- [17] J. Eberth, H. G. Thomas, P. v. Brentano, R. M. Lieder, H. M. Jäger, H. Kämmerling, M. Berst, D. Gutknecht, and R. Henck, *Nucl. Instrum. Methods Phys. Res., Sect. A* **369**, 135 (1996).
- [18] W. Kurcewicz, E. F. Zganjar, R. Kirchner, O. Klepper, E. Roeckl, P. Komninos, E. Nolte, D. Schardt, and P. Tidemand-Petersson, *Z. Phys. A* **308**, 21 (1982).
- [19] L. Cáceres *et al.*, *Phys. Rev. C* **79**, 011301 (2009).
- [20] A. de Shalit and I. Talmi, *Nuclear Shell Theory* (Academic Press, New York, 1963), p. 315.
- [21] T. Faestermann, M. Górski, and H. Grawe, *Prog. Part. Nucl. Phys.* **69**, 85 (2013).
- [22] R. Grzywacz *et al.*, *Phys. Rev. Lett.* **81**, 766 (1998).
- [23] C. Mazzocchi *et al.*, *Phys. Lett. B* **622**, 45 (2005).
- [24] M. Sawicka *et al.*, *Phys. Rev. C* **68**, 044304 (2003).
- [25] A. F. Lisetskiy, B. A. Brown, M. Horoi, and H. Grawe, *Phys. Rev. C* **70**, 044314 (2004).
- [26] P. V. Isacker, *J. Phys. Conf. Ser.* **322**, 012003 (2011).
- [27] C. J. Chiara *et al.*, *Phys. Rev. C* **84**, 037304 (2011).
- [28] <http://www.nndc.bnl.gov/ensdf/>.
- [29] A. Blazhev *et al.*, *Phys. Rev. C* **69**, 064304 (2004).